The transverse spin-1 Ising film

2000 J. Phys.: Condens. Matter 12 43

(http://iopscience.iop.org/0953-8984/12/1/304)

J. Phys.: Condens. Matter **12** (2000) 43–53. Printed in the UK PII: S0953-8984(00)04096-0

The transverse spin-1 Ising film

A Saber†‡, A Ainane†‡, F Dujardin†, N El Aouad‡, M Saber†‡ and B Stébé†

† Laboratoire de Théorie de la Matière Condensée, Université de Metz, Institut de Physique et d'Electronique, 1, Boulevard Arago, 57078 Metz Cedex 3, France

‡ Département de Physique, Faculté des Sciences, Université Moulay Ismail, BP 4010, Meknès, Morocco

Received 17 May 1999, in final form 15 October 1999

Abstract. Within the framework of the effective-field theory, we examine the phase transitions of a transverse spin-1 Ising film. We discuss an L-layer film of simple cubic symmetry with nearest-neighbour exchange interactions in which the exchange interaction strengths in surface layers are assumed to be different from the bulk values, and we derive and illustrate expressions for the phase diagrams and order parameter profiles. It is found that for a ratio of the surface exchange interactions to the bulk ones $R = J_s/J$ less than a critical value R_c, the critical temperature T_c/J of the film is smaller than the bulk critical temperature T_c^B/J and, as L is increased further, T_c/J increases. However, for $R > R_c$, T_c/J is greater than the bulk critical temperature T_c^B/J and, as L is increased further, T_c/J decreases.

1. Introduction

The magnetic properties of ordinary lattices, thin films, multilayers and artificially fabricated superlattices have been widely studied over the years [1]. It is generally accepted that the magnetic properties of a surface layer may differ from those in the bulk of the system. This is expected since the atoms in the surface layer or region are in a different environment and the exchange interactions associated with them may differ from those in the bulk.

In the case of spin waves, the presence of a surface with different interactions gives rise to the existence of surface spin waves [2–6]. These spin waves are localized at the surfaces and have been studied in the magnetostatic approach [2–6]. In the case of phase transitions, it has also been recognized that the presence of a surface raises the possibility of a surface transition. Here the surface layer orders at a temperature $T_c^S > T_c^B$ (T_c^B is the bulk critical temperature) and in the temperature region $T_c^B < T < T_c^S$ the magnetization decays from the surface into the bulk with a characteristic length. This occurs when the ratio of the surface exchange interaction to the bulk one $R = J_s/J$ is larger than a critical value R_c.

From both the experimental and the theoretical points of view, the Ising magnetic film is very important [7–10]. It can be taken as a model to investigate the magnetic size effects and can be regarded as a quasi-two-dimensional system when it is thin [9]. The magnetic properties of the film will approach those of the corresponding semi-infinite system when it is thick [10]. Although much is known about phase transitions in two- and three-dimensional systems, many aspects remain to be understood in systems with surfaces, thin films etc. Very often one finds unexpected and interesting properties in these systems. For example, experimental studies [11–15] on the magnetic properties of surfaces of Gd, Cr and Tb have shown that a surface ordered magnetically can coexist with a magnetically disordered bulk phase.

0953-8984/00/010043+11$30.00

In this paper, we are concerned with order–disorder (KDP-like) ferroelectrics. As was first pointed out by de Gennes [15], these may be described within a pseudo-spin model by the Ising model in a transverse field since the phase transition to ferroelectricity is associated with preferential occupation by the protons of one or the other of the two equivalent wells in the hydrogen bonds. By modifying the exchange interaction and the transverse field at the surface, Wang *et al* [16] successfully extended the transverse Ising model to the study of surface and size effects in ferroelectric films. The polarization, the critical temperature as well as the phase diagram as functions of exchange interactions, transverse fields and film thicknesses are investigated [16–19]. The transverse Ising model has also been applied to many other systems, such as the semi-infinite systems of localized surface spin waves [20] and surface magnetism [21]. All the studies mentioned above are concerned with Ising systems with spin of magnitude $\frac{1}{2}$. In addition, there have been few studies of the critical and magnetic properties of the transverse Ising film with a higher spin. To our knowledge, only Benyoussef *et al* [22], using the mean-field approximation, have studied the semi-infinite spin-1 Ising model and Saber *et al* [23], within the framework of the effective-field theory, with a probability distribution technique [24], have investigated the order parameter behaviour of a transverse Ising ferromagnetic thin film with spin-1.

Our aim here is to study the order parameter profiles and the phase diagrams of the transverse spin-1 Ising film, using the effective-field theory.

In the following section, we introduce the model and derive the order parameter profiles, with a description of the calculation of the phase diagrams. The presentation of the numerical results and their discussion is contained in section 3. The last section, section 4, is devoted to conclusions.

2. Formalism

The system to be treated is a transverse spin-1 Ising film having a simple cubic structure with (001) and $(00L)$ surfaces with L layers in the z-direction (the same as that studied in reference [23]). The Hamiltonian of the system is given by

$$H = -\sum_{(i,j)} J_{ij} S_{iz} S_{jz} - \Omega \sum_{i} S_{ix} \tag{1}$$

where S_{iz} and S_{ix} denote the z- and x-components of a quantum spin $\vec{S}_i$ of magnitude $S = 1$ at site i, Ω represents the transverse field and J_{ij} is the strength of the exchange interaction between the spins at nearest-neighbour sites i and j. $J_{ij} = J_s$ if both spins are in surface layers and $J_{ij} = J$ otherwise.

The statistical properties of the system were studied using an effective-field theory in reference [23]. The layer longitudinal magnetizations are given by

$$\begin{aligned} m_{1z} = 2^{-N-N_0} & \sum_{\mu=0}^{N} \sum_{\nu=0}^{N-\mu} \sum_{\mu_1=0}^{N_0} \sum_{\nu_1=0}^{N_0-\mu_1} 2^{\mu+\mu_1} C_{\mu}^{N} C_{\nu}^{N-\mu} C_{\mu_1}^{N_0} C_{\nu_1}^{N_0-\mu_1} \\ & \times (1-2q_{1z})^{\mu} (q_{1z} - m_{1z})^{\nu} (q_{1z} + m_{1z})^{N-\mu-\nu} \\ & \times (1-2q_{2z})^{\mu_1} (q_{2z} - m_{2z})^{\nu_1} (q_{2z} + m_{2z})^{N_0-\mu_1-\nu_1} \\ & \times f_{1z}(y_1, \Omega/J) \end{aligned} \tag{2}$$

$$\vdots$$

$$m_{nz} = 2^{-N-2N_0} \sum_{\mu=0}^{N} \sum_{\nu=0}^{N-\mu} \sum_{\mu_1=0}^{N_0} \sum_{\nu_1=0}^{N_0-\mu_1} \sum_{\mu_2=0}^{N_0} \sum_{\nu_2=0}^{N_0-\mu_2} 2^{\mu+\mu_1+\mu_2} C_\mu^N C_\nu^{N-\mu} C_{\mu_1}^{N_0} C_{\nu_1}^{N_0-\mu_1} C_{\mu_2}^{N_0} C_{\nu_2}^{N_0-\mu_2}$$
$$\times (1-2q_{nz})^\mu (q_{nz}-m_{nz})^\nu (q_{nz}+m_{nz})^{N-\mu-\nu}$$
$$\times (1-2q_{n-1,z})^{\mu_1} (q_{n-1,z}-m_{n-1,z})^{\nu_1} (q_{n-1,z}+m_{n-1,z})^{N_0-\mu_1-\nu_1}$$
$$\times (1-2q_{n+1,z})^{\mu_2} (q_{n+1,z}-m_{n+1,z})^{\nu_2} (q_{n+1,z}+m_{n+1,z})^{N_0-\mu_2-\nu_2}$$
$$\times f_{1z}(y_n, \Omega/J) \qquad \text{for } n = 2, 3, \ldots, L-1 \tag{3}$$

$$\vdots$$

$$m_{Lz} = 2^{-N-N_0} \sum_{\mu=0}^{N} \sum_{\nu=0}^{N-\mu} \sum_{\mu_1=0}^{N_0} \sum_{\nu_1=0}^{N_0-\mu_1} 2^{\mu+\mu_1} C_\mu^N C_\nu^{N-\mu} C_{\mu_1}^{N_0} C_{\nu_1}^{N_0-\mu_1}$$
$$\times (1-2q_{Lz})^\mu (q_{Lz}-m_{Lz})^\nu (q_{Lz}+m_{Lz})^{N-\mu-\nu}$$
$$\times (1-2q_{L-1,z})^{\mu_1} (q_{L-1,z}-m_{L-1,z})^{\nu_1} (q_{L-1,z}+m_{L-1,z})^{N_0-\mu_1-\nu_1}$$
$$\times f_{1z}(y_L, \Omega/J) \tag{4}$$

where

$$y_1 = y_L = R(N-\mu-2\nu) + (N_0-\mu_1-2\nu_1)$$
$$y_n = (N-\mu-2\nu) + (N_0-\mu_1-2\nu_1) + (N_0-\mu_2-2\nu_2) \qquad \text{for } n = 2, 3, \ldots, L-1$$

and

$$f_{1z}(y, \Omega/J) = \frac{2y}{[y^2+(\Omega/J)^2]^{1/2}} \frac{2\sinh(\beta J[y^2+(\Omega/J)^2]^{1/2})}{1+2\cosh(\beta J[y^2+(\Omega/J)^2]^{1/2})}. \tag{5}$$

In these equations, we have introduced $R = J_s/J$, N and N_0 are the numbers of nearest neighbours in the plane and between adjacent planes respectively ($N = 4$ and $N_0 = 1$ in the case of a simple cubic lattice which is considered here) and C_k^l are the binomial coefficients, $C_k^l = l!/(k!(l-k)!)$.

The equations for the longitudinal quadrupolar moments are obtained by substituting for the function f_{1z} with f_{2z} in the expressions for the layer longitudinal magnetizations. This yields

$$q_{nz} = m_{nz}[f_{1z}(y_n, \Omega/J) \to f_{2z}(y_n, \Omega/J)] \tag{6}$$

where

$$f_{2z}(y, \Omega) = \frac{1}{[y^2+\Omega^2]} \frac{\Omega^2 + (2y^2+\Omega^2)\cosh(\beta[y^2+\Omega^2]^{1/2})}{1+2\cosh(\beta[y^2+\Omega^2]^{1/2})}. \tag{7}$$

The longitudinal magnetization and quadrupolar moment of the film are defined as the averages of layer ones and they are given by

$$\bar{m}_z = \frac{1}{L} \sum_{n=1}^{L} m_{nz} \tag{8}$$

$$\bar{q}_z = \frac{1}{L} \sum_{n=1}^{L} q_{nz}. \tag{9}$$

In this work we are interested in the calculation of the longitudinal ordering near the transition critical temperature. The usual argument that m_{nz} tends to zero as the temperature approaches its critical value allows us to consider only terms linear in m_{nz} because higher-order terms tend to zero faster than m_{nz} on approaching a critical temperature. Consequently, all terms of order higher than linear terms in equations (2)–(4) which give the expressions for m_{nz} can be neglected. This leads to the set of simultaneous equations

$$m_{nz} = A_{n,n-1}m_{n-1,z} + A_{n,n}m_{nz} + A_{n,n+1}m_{n+1,z} \tag{10}$$

or

$$\mathbf{A}\vec{m}_z = \vec{m}_z \tag{11}$$

where $\vec{m}_z$ is a vector of components $(m_{1z}, m_{2z}, \ldots, m_{nz}, \ldots, m_{Lz})$ and the matrix $\mathbf{A}$ is symmetric and tridiagonal with elements

$$A_{i,j} = A_{i,i}\delta_{i,j} + A_{i,j}(\delta_{i,j-1} + \delta_{i,j+1}). \tag{12}$$

The system of equations (10) is of the form

$$\mathbf{M}\vec{m}_z = 0 \tag{13}$$

where

$$M_{i,j} = (1 - A_{i,i})\delta_{i,j} - A_{i,j}(\delta_{i,j-1} + \delta_{i,j+1}). \tag{14}$$

All of the information about the critical temperature of the system is contained in equation (13). Up to know we have not used precise values of the exchange interactions and the transverse field; the terms in matrix (13) are general ones.

In a general case, for arbitrary exchange interactions, transverse field and film thickness the evaluation of the critical temperature relies on numerical solution of the system of linear equations (13). These equations are fulfilled if and only if

$$\det \mathbf{M} = 0 \tag{15}$$

where

$$\det \mathbf{M} = \alpha \begin{vmatrix} a_1 & -1 & & & & \\ -1 & a_2 & -1 & & & \\ \cdots & \cdots & \cdots & \cdots & \cdots & \cdots \\ & & -1 & a_n & -1 & \\ \cdots & \cdots & \cdots & \cdots & \cdots & \cdots \\ & & & -1 & a_{L-1} & -1 \\ & & & & -1 & a_L \end{vmatrix}_L . \tag{16}$$

The parameters $\alpha, a_1, a_2, \ldots$ and a_L that appear in equation (16) are given by

$$\alpha = A_{1,2}A_{2,1}\cdots A_{n,n-1}A_{n,n+1}\cdots A_{L-1,L-2}A_{L-1,L}A_{L,L-1} \tag{17}$$

$$a_1 = \frac{1 - A_{1,1}}{A_{1,2}} \tag{18}$$

$$\vdots$$

$$a_n = \frac{1 - A_{n,n}}{A_{n,n-1}} = \frac{1 - A_{n,n}}{A_{n,n+1}} = \frac{1 - A_{n,n}}{A_{n,n}/4} \qquad \text{for } n = 2, 3, \ldots, L-1 \tag{19}$$

$$\vdots$$

$$a_L = \frac{1 - A_{L,L}}{A_{L,L-1}}. \tag{20}$$

In general equation (16) can be satisfied for L different values of the critical temperature T_c/J from which we choose the one corresponding to the highest possible transition temperature (see the discussion in references [25, 26]). This value of T_c/J corresponds to a solution having $m_{1z}, m_{2z}, \ldots, m_{Lz}$ positive, which is compatible with a ferromagnetic longitudinal ordering. The other formal solutions correspond in principle to other types of ordering that usually do not occur here (see Ferchmin and Maciejewski [26]).

3. Results and discussion

Throughout this paper, we take J as the unit of energy, and the length is measured in units of the lattice constant in our numerical calculations. From equation (15), we can obtain the phase diagrams of the film. The results show that there can be two phases, a film ferromagnetic phase (F) which means that the longitudinal magnetization in the film

$$\bar{m}_z = \frac{1}{L}\sum_{n=1}^{L} m_{nz}$$

is different from zero, and a film paramagnetic phase (P) which corresponds to $\bar{m}_z = 0$.

First we calculate the $(T_c/J, R = J_s/J)$ phase diagrams for different transverse fields and numbers of layers. Typical results can be seen in figure 1 where the solid, dashed and dotted lines correspond respectively to $\Omega/J = 0$, 2 and 4. For each value of Ω/J, we see that all the curves intersect at the same abscissa point $R = R_c = 1.294$ and ordinate point $T_c/J = (T_c^B/J)(\Omega/J) = 3.519$, 3.323 and 2.599 for $\Omega/J = 0$, 2 and 4 respectively. According to these results, the parameter R_c can be defined as that particular R-value at which the critical temperature does not depend on the film thickness (the crossover point in figure 1). Furthermore, according to the definition of R_c, the crossover point in figure 1 can be expected to define also the critical temperature of the three-dimensional infinite bulk system, where the surfaces (001) and (00L) and the R-parameter are of no importance. For $R < R_c$, the critical temperature T_c/J of the film is smaller than the bulk critical temperature T_c^B/J of the

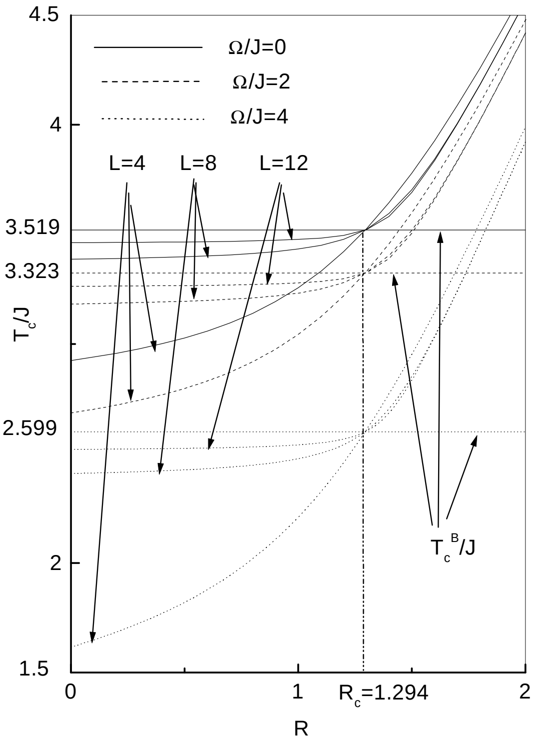

Figure 1. The phase diagram in the $(T_c/J, R = J_s/J)$ plane. The solid, dashed and dotted lines correspond respectively to $\Omega/J = 0$, 2 and 4. The number accompanying each curve denotes the value of the thickness L of the film.

corresponding bulk transverse Ising system. T_c/J increases with L and approaches the bulk critical temperature $T_c^B/J = (T_c^B/J)(\Omega/J)$ asymptotically as the number of layers becomes large. When $R = R_c$, the critical temperature of the film T_c/J is independent of L, and equal to T_c^B/J. On the other hand, for $R > R_c$ the critical temperature of the film T_c/J is greater both than T_c^B/J and than T_c^S/J (the bulk and surface critical temperatures of the corresponding semi-infinite Ising system) and the larger L is, the lower T_c/J is. T_c/J approaches the surface critical temperature T_c^S/J of the corresponding semi-infinite Ising system for large values of L. This figure shows also that the critical value R_c of the parameter R is independent of the strength of the transverse field Ω/J and the presence of the transverse field causes only a reduction in the critical temperatures.

In figure 2, we present the bulk critical temperature together with the critical temperature of the film as a function of the strength of the transverse field Ω/J for different thicknesses L and for two values of the parameter R, i.e., $R = 0.1 < R_c$ (solid curves) and $R = 2 > R_c$ (dotted curves). The dashed line is the bulk critical temperature T_c^B/J. The presence of a transverse field, of course, causes a reduction in the critical temperatures. We find that the $(T_c/J, \Omega/J)$ curve for a given value of R and the (Ω/J)-axis intersect at some critical point, and the value of Ω/J corresponding to this point is called the critical transverse field Ω_c/J. When $\Omega/J > \Omega_c/J$, at any temperature, there cannot be a ferromagnetic phase. For $R = 0.1 < R_c$, we see from this figure that the critical temperature T_c/J of the film is less than the bulk critical temperature T_c^B/J and it increases with the increase of L to approach

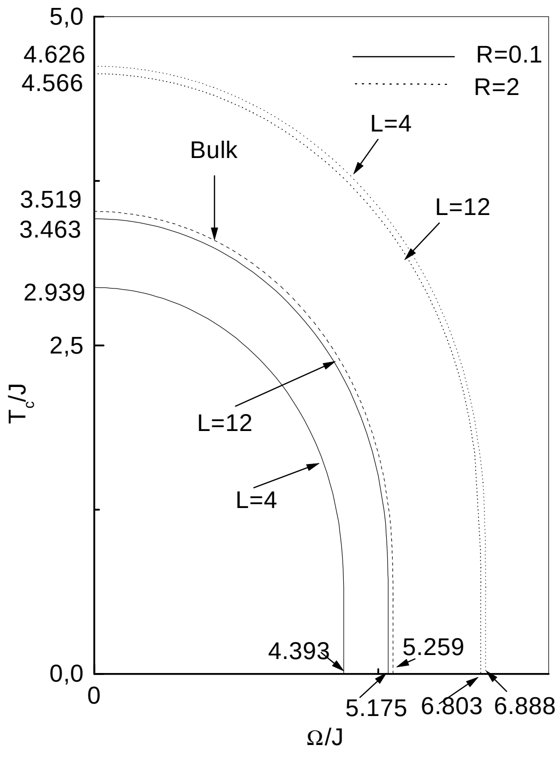

Figure 2. The phase diagram in the $(T_c/J, \Omega/J)$ plane. The solid and dotted curves correspond respectively to $R = 0.1$ and 2. The dashed line is the bulk critical temperature T_c^B/J. The number accompanying each curve denotes the value of the thickness L of the film.

asymptotically T_c^B/J for large values of L. For $R = 2 > R_c$, T_c/J is greater than T_c^B/J and it decreases with the increase of L to approach asymptotically a critical temperature which depends on R for large values of L (the surface critical temperature T_c^S/J of the corresponding semi-infinite Ising system).

We present in figure 3 the dependence of the bulk critical temperature and the critical temperature of the film for different values of R and for two values of the strength of the transverse field $\Omega/J = 0$ (solid curves) and $\Omega/J = 4$ (dotted curves). For a given value of Ω/J, this figure shows that for any value of the parameter R below $R_c = 1.294$, the film critical temperature T_c/J is smaller than $T_c^B/J = (T_c^B/J)(\Omega/J)$ and it increases with the increase of the film thickness L to approach T_c^B/J. When $R = R_c$, T_c/J is independent of L and T_c/J is equal to T_c^B/J. For $R > R_c$, we see that T_c/J is greater than T_c^B/J and it decreases with the increase of the film thickness L to approach asymptotically a critical temperature depending on R when the number of layers becomes large.

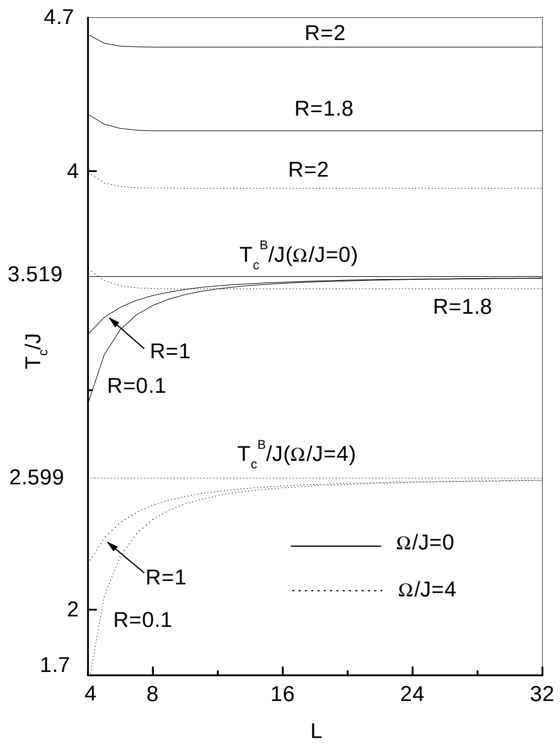

Figure 3. The thickness dependence of the critical temperature of the film. The solid and dotted lines correspond respectively to $\Omega/J = 0$ and 4. The number accompanying each curve denotes the value of the parameter R.

We now turn to the study of the longitudinal magnetization m_{nz} and quadrupolar moment q_{nz} for a film with L layers. After selecting a value of the strength of the transverse field Ω/J, a value of the ratio of the surface exchange interactions to the bulk ones (the parameter R) and a value of the film thickness L, we can obtain the layer longitudinal magnetization and quadrupolar moment from equations (2)–(4) and (6) as functions of temperature.

In figure 4, we show the longitudinal magnetization (m_{nz}) and quadrupolar moment (q_{nz}) profiles for a film with $L = 40$ layers. They are drawn for a fixed value of the strength of the transverse field $\Omega/J = 4$ and for a fixed value of the parameter $R = 0.1 < R_c$. The solid and

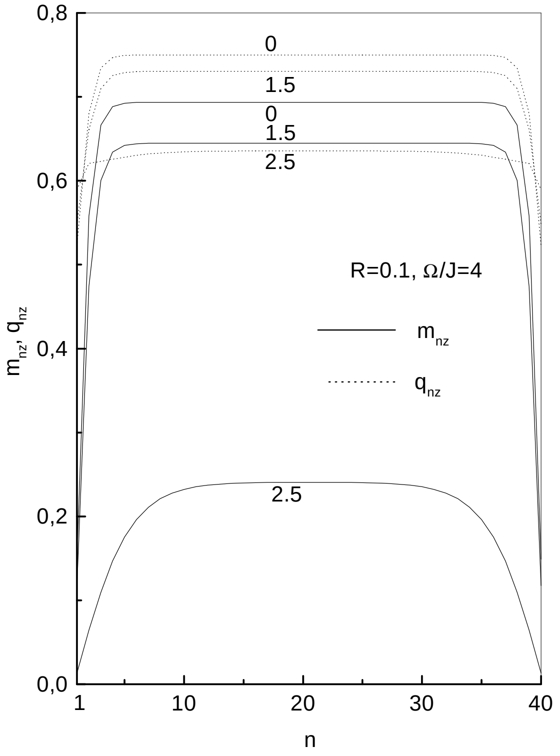

Figure 4. Longitudinal magnetization and quadrupolar moment profiles for a film with $L = 40$ layers when $R = 0.1$ and $\Omega/J = 4$. The solid and dotted lines correspond respectively to m_{nz} and q_{nz}. The number accompanying each curve denotes the value of the temperature T/J.

dotted curves correspond respectively to m_{nz} and q_{nz}. The number accompanying each curve denotes the value of the temperature T/J. Because of the symmetry of the film, we limit the interpretation to the first half of the layers. We see that the film longitudinal magnetization m_{nz} and quadrupolar moment q_{nz} have their smallest values at the surfaces and they increase with the number of layers to reach their maximal values in the bulk ($n = 20$). m_{nz} and q_{nz} decrease with the increase of the temperature T/J as expected.

Figure 5 shows the longitudinal magnetization (m_{nz}) and quadrupolar moment (q_{nz}) profiles for a film with $L = 40$ layers. They are drawn for a fixed value of the strength of the transverse field $\Omega/J = 4$ and for a fixed value of the parameter $R = 2 > R_c$. We see that the film longitudinal magnetization m_{nz} and quadrupolar moment q_{nz} have their largest values at the surfaces and they decrease with the number of layers to reach their minimal values in the bulk ($n = 20$). m_{nz} and q_{nz} decrease with the increase of the temperature T/J as expected.

4. Conclusions

In summary, we have studied the phase diagrams and the longitudinal magnetization and quadrupolar moment profiles of the transverse spin-1 Ising film where the exchange interactions between spins at the surfaces are different from the exchange interactions between spins in the bulk within the effective-field theory. The effects of the ratio $R = J_s/J$ of the surface

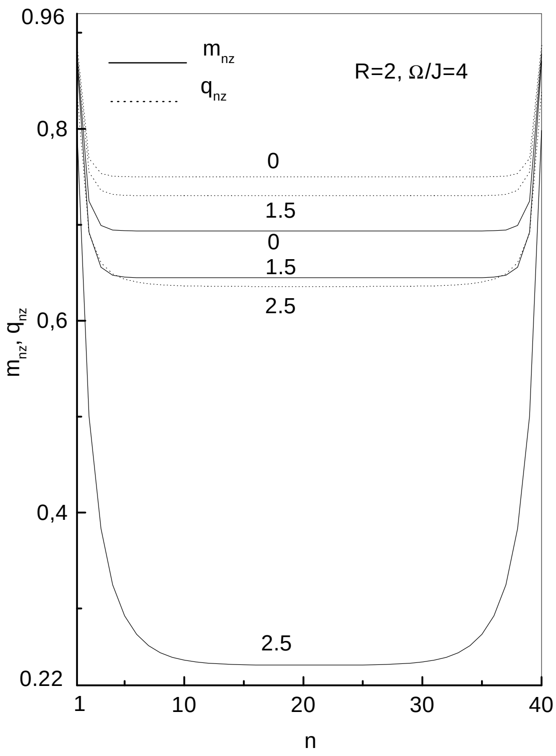

Figure 5. Longitudinal magnetization and quadrupolar moment profiles for a film with $L = 40$ layers when $R = 2$ and $\Omega/J = 4$. The solid and dotted lines correspond respectively to m_{nz} and q_{nz}. The number accompanying each curve denotes the value of the temperature T/J.

exchange interactions to the bulk ones, the strength of the transverse field Ω/J and the film thickness L on the phase diagrams are investigated. Some interesting properties have been found. The results are in agreement with those found earlier in [23]. They are as follows.

(i) There is a critical value $R_c = 1.294$ independent of the strength of the transverse field. For a given value of Ω/J: when $R < R_c$, as the film thickness increases, the film critical temperature T_c/J increases; when $R > R_c$, as the film thickness increases, the film critical temperature T_c/J decreases. However, for $R = R_c$, T_c/J is independent of the film thickness L and T_c/J is equal to T_c^B/J.

(ii) The film longitudinal magnetization $\bar{m}_z$ and quadrupolar moment $\bar{q}_z$ decrease with the increase of L for $R > R_c$, increase with the increase of L for $R < R_c$ and are equal to their corresponding bulk values m_z^B and q_z^B for $R = R_c$.

Acknowledgments

This work was initiated with the PARS: PHYSIQUE 22 and completed during a visit of AS, AA and MS to the Université de Metz, France, in the framework of the 'Action Intégrée No 46/SM/97'.

Appendix A

The only non-zero elements of the matrix **A** are given by

$$A_{1,1} = 2^{-N-N_0} \sum_{\mu=0}^{N} \sum_{\nu=0}^{N-\mu} \sum_{\mu_1=0}^{N_0} \sum_{\nu_1=0}^{N_0-\mu_1} \sum_{i=0}^{\nu} \sum_{j=0}^{N-(\mu+\nu)} (-1)^i 2^{\mu+\mu_1} \delta_{1,i+j} \times C_\mu^N C_\nu^{N-\mu} C_{\mu_1}^{N_0} C_{\nu_1}^{N_0-\mu_1} C_i^\nu C_j^{N-(\mu+\nu)} (1-r_1)^\mu \times (1-r_2)^{\mu_1} r_1^{(N-\mu)-(i+j)} r_2^{N_0-\mu_1} f_{1z}(y_1, \Omega/J) \quad (A.1)$$

$$A_{1,2} = 2^{-N-N_0} \sum_{\mu=0}^{N} \sum_{\nu=0}^{N-\mu} \sum_{\mu_1=0}^{N_0} \sum_{\nu_1=0}^{N_0-\mu_1} \sum_{i=0}^{\nu_1} \sum_{j=0}^{N_0-(\mu_1+\nu_1)} (-1)^i 2^{\mu+\mu_1} \delta_{1,i+j} \times C_\mu^N C_\nu^{N-\mu} C_{\mu_1}^{N_0} C_{\nu_1}^{N_0-\mu_1} C_i^{\nu_1} C_j^{N_0-(\mu_1+\nu_1)} (1-r_1)^\mu \times (1-r_2)^{\mu_1} r_1^{N-\mu} r_2^{(N_0-\mu_1)-(i+j)} f_{1z}(y_1, \Omega/J) \quad (A.2)$$

$$\vdots$$

$$A_{n,n-1} = 2^{-N-2N_0} \sum_{\mu=0}^{N} \sum_{\nu=0}^{N-\mu} \sum_{\mu_1=0}^{N_0} \sum_{\nu_1=0}^{N_0-\mu_1} \sum_{\mu_2=0}^{N_0} \sum_{\nu_2=0}^{N_0-\mu_2} \sum_{i=0}^{\nu_1} \sum_{j=0}^{N_0-(\mu_1+\nu_1)} (-1)^i 2^{\mu+\mu_1+\mu_2} \delta_{1,i+j} \times C_\mu^N C_\nu^{N-\mu} C_{\mu_1}^{N_0} C_{\nu_1}^{N_0-\mu_1} C_{\mu_2}^{N_0} C_{\nu_2}^{N_0-\mu_2} C_i^{\nu_1} C_j^{N_0-(\mu_1+\nu_1)} (1-r_n)^\mu \times (1-r_{n-1})^{\mu_1} (1-r_{n+1})^{\mu_2} r_n^{N-\mu} r_{n-1}^{(N_0-\mu_1)-(i+j)} r_{n+1}^{N_0-\mu_2} f_{1z}(y_n, \Omega/J) \quad (A.3)$$

$$A_{n,n} = 2^{-N-2N_0} \sum_{\mu=0}^{N} \sum_{\nu=0}^{N-\mu} \sum_{\mu_1=0}^{N_0} \sum_{\nu_1=0}^{N_0-\mu_1} \sum_{\mu_2=0}^{N_0} \sum_{\nu_2=0}^{N_0-\mu_2} \sum_{i=0}^{\nu} \sum_{j=0}^{N-(\mu+\nu)} (-1)^i 2^{\mu+\mu_1+\mu_2} \delta_{1,i+j} \times C_\mu^N C_\nu^{N-\mu} C_{\mu_1}^{N_0} C_{\nu_1}^{N_0-\mu_1} C_{\mu_2}^{N_0} C_{\nu_2}^{N_0-\mu_2} C_i^{\nu} C_j^{N-(\mu+\nu)} (1-r_n)^\mu \times (1-r_{n-1})^{\mu_1} (1-r_{n+1})^{\mu_2} r_n^{(N-\mu)-(i+j)} r_{n-1}^{N_0-\mu_1} r_{n+1}^{N_0-\mu_2} f_{1z}(y_n, \Omega/J) \quad (A.4)$$

$$A_{n,n+1} = 2^{-N-2N_0} \sum_{\mu=0}^{N} \sum_{\nu=0}^{N-\mu} \sum_{\mu_1=0}^{N_0} \sum_{\nu_1=0}^{N_0-\mu_1} \sum_{\mu_2=0}^{N_0} \sum_{\nu_2=0}^{N_0-\mu_2} \sum_{i=0}^{\nu_2} \sum_{j=0}^{N_0-(\mu_2+\nu_2)} (-1)^i 2^{\mu+\mu_1+\mu_2} \delta_{1,i+j} \times C_\mu^N C_\nu^{N-\mu} C_{\mu_1}^{N_0} C_{\nu_1}^{N_0-\mu_1} C_{\mu_2}^{N_0} C_{\nu_2}^{N_0-\mu_2} C_i^{\nu_2} C_j^{N_0-(\mu_2+\nu_2)} (1-r_n)^\mu \times (1-r_{n-1})^{\mu_1} (1-r_{n+1})^{\mu_2} r_n^{N-\mu} r_{n-1}^{N_0-\mu_1} r_{n+1}^{(N_0-\mu_2)-(i+j)} f_{1z}(y_n, \Omega/J) \quad (A.5)$$

$$\vdots$$

$$A_{L,L-1} = 2^{-N-N_0} \sum_{\mu=0}^{N} \sum_{\nu=0}^{N-\mu} \sum_{\mu_1=0}^{N_0} \sum_{\nu_1=0}^{N_0-\mu_1} \sum_{i=0}^{\nu_1} \sum_{j=0}^{N_0-(\mu_1+\nu_1)} (-1)^i 2^{\mu+\mu_1} \delta_{1,i+j} \times C_\mu^N C_\nu^{N-\mu} C_{\mu_1}^{N_0} C_{\nu_1}^{N_0-\mu_1} C_i^{\nu_1} C_j^{N_0-(\mu_1+\nu_1)} (1-r_L)^\mu \times (1-r_{L-1})^{\mu_1} r_L^{N-\mu} r_{L-1}^{(N_0-\mu_1)-(i+j)} f_{1z}(y_L, \Omega/J) \quad (A.6)$$

$$A_{L,L} = 2^{-N-N_0} \sum_{\mu=0}^{N} \sum_{\nu=0}^{N-\mu} \sum_{\mu_1=0}^{N_0} \sum_{\nu_1=0}^{N_0-\mu_1} \sum_{i=0}^{\nu} \sum_{j=0}^{N-(\mu+\nu)} (-1)^i 2^{\mu+\mu_1} \delta_{1,i+j} \times C_\mu^N C_\nu^{N-\mu} C_{\mu_1}^{N_0} C_{\nu_1}^{N_0-\mu_1} C_i^{\nu} C_j^{N-(\mu+\nu)} (1-r_L)^\mu \times (1-r_{L-1})^{\mu_1} r_L^{(N-\mu)-(i+j)} r_{L-1}^{N_0-\mu_1} f_{1z}(y_L, \Omega/J) \quad (A.7)$$

where the r_n are the values of the q_{nz} when $m_{nz} = 0$ at the critical point which are given by

$$r_1 = 2^{-N-N_0} \sum_{\mu=0}^{N} \sum_{\nu=0}^{N-\mu} \sum_{\mu_1=0}^{N_0} \sum_{\nu_1=0}^{N_0-\mu_1} 2^{\mu+\mu_1} C_\mu^N C_\nu^{N-\mu} C_{\mu_1}^{N_0} C_{\nu_1}^{N_0-\mu_1} \times (1-2r_1)^\mu r_1^{N-\mu} (1-2r_2)^{\mu_1} r_2^{N_0-\mu_1} f_{2z}(y_1, \Omega/J) \tag{A.8}$$

$$\vdots$$

$$r_n = 2^{-N-2N_0} \sum_{\mu=0}^{N} \sum_{\nu=0}^{N-\mu} \sum_{\mu_1=0}^{N_0} \sum_{\nu_1=0}^{N_0-\mu_1} \sum_{\mu_2=0}^{N_0} \sum_{\nu_2=0}^{N_0-\mu_2} 2^{\mu+\mu_1+\mu_2} C_\mu^N C_\nu^{N-\mu} \times C_{\mu_1}^{N_0} C_{\nu_1}^{N_0-\mu_1} C_{\mu_2}^{N_0} C_{\nu_2}^{N_0-\mu_2} (1-2r_n)^\mu r_n^{N-\mu} (1-2r_{n-1})^{\mu_1} r_{n-1}^{N_0-\mu_1} \times (1-2r_{n+1})^{\mu_2} r_{n+1}^{N_0-\mu_2} f_{2z}(y_n, \Omega/J) \qquad \text{for } n = 2, 3, \ldots, L-1 \tag{A.9}$$

$$\vdots$$

$$r_L = 2^{-N-N_0} \sum_{\mu=0}^{N} \sum_{\nu=0}^{N-\mu} \sum_{\mu_1=0}^{N_0} \sum_{\nu_1=0}^{N_0-\mu_1} 2^{\mu+\mu_1} C_\mu^N C_\nu^{N-\mu} C_{\mu_1}^{N_0} C_{\nu_1}^{N_0-\mu_1} \times (1-2r_L)^\mu r_L^{N-\mu} (1-2r_{L-1})^{\mu_1} r_{L-1}^{N_0-\mu_1} f_{2z}(y_L, \Omega/J). \tag{A.10}$$

References

[1] Bruno E and Gyorffy B L 1994 *Appl. Surf. Sci.* **75** 320
[2] For a review, see Cottam M G and Tilley D R (ed) 1989 *Introduction to Surface and Superlattice Excitations* (Cambridge: Cambridge University Press)
[3] Camely R E, Rahman T S and Mills D L 1983 *Phys. Rev.* B **27** 261
[4] Grunberg P and Mika K 1983 *Phys. Rev.* B **27** 2955
[5] Hillebrands B 1990 *Phys. Rev.* B **41** 530
[6] Sy H K and Chen F 1994 *Phys. Rev.* B **50** 3411
[7] Ferchmin A R 1982 *IEEE Trans. Magn.* **18** 714
[8] Mielnicki J, Balcerzak T and Wiatrowski G 1987 *J. Magn. Magn. Mater.* **65** 27
[9] Barber M N 1983 *Phase Transitions and Critical Phenomena* vol 8, ed C Domb and J L Lebowitz (New York: Acadenic)
[10] Saber M, Ainane A, Dujardin F and Stébé B 1999 *Phys. Rev.* B **59** 6908
[11] Rau C and Eichner S 1980 *Nuclear Methods in Materials Research* ed K Bethege, H Bauman, H Hex and F Rauch (Braunschweig: Vieweg) p 354
[12] Weller D, Alvarado S F, Gudat W, Schroder K and Capagna M 1985 *Phys. Rev. Lett.* **54** 1555
[13] Rau C and Eichner S 1981 *Phys. Rev. Lett.* **47** 939
[14] Rau C, Jin C and Robert M 1988 *J. Appl. Phys.* **63** 3667
[15] de Gennes P G 1963 *Solid State Commun.* **1** 132
[16] Wang C L, Zhong W L and Zhang P L 1992 *J. Phys.: Condens. Matter* **3** 4743
[17] Sy H K 1993 *J. Phys.: Condens. Matter* **5** 1213
[18] Ainane A, Dujardin F, Saber M and Stébé 1999 *Physica* A **262** 518
[19] Cottam M G, Tilley D R and Zeks B 1984 *J. Phys. C: Solid State Phys.* **17** 1793
[20] Tamura I, Sarmento E F and Kaneyoshi T 1984 *J. Phys. C: Solid State Phys.* **17** 3207
[21] Kaneyoshi T 1991 *Introduction to Surface Magnetism* (Boca Raton, FL: Chemical Rubber Company Press)
[22] Benyoussef A, Boccara N and Saber M 1986 *J. Phys. C: Solid State Phys.* **19** 1983
[23] Saber A, Ainane A, Dujardin F, Saber M and Stébé B 1999 *J. Phys.: Condens. Matter* **11** 2087
[24] Tucker J W, Saber M and Peliti L 1994 *Physica* A **206** 497
[25] Corciovei A, Gostache G and Vamanu D 1972 *Solid State Physics* ed H Ehrenreich, F Seitz and D Turnbull (New York: Academic) p 237
[26] Ferchmin A R and Maciejewski W 1979 *J. Phys. C: Solid State Phys.* **12** 4311